International Journal of Engineering Science Invention (IJESI)
ISSN (Online): 2319 – 6734, ISSN (Print): 2319 – 6726
www.ijesi.org ||Volume 7 Issue 9 Ver III || Sep 2018 || PP 13-22

Simulation of Flow Behaviour around Bridge Piers Using ANSYS – CFD

Prasanna S V S N D L[1], and Suresh Kumar, N.[2]
[1 ,2] *(Department of Civil Engg., College of Engg (A), Osmania University, Hyderabad-500 007, India)*
Corresponding Author; Prasanna S V S N D L

Abstract: *The threat of local scour around bridge piers has been in research for many years. According to the various studies, local scour around the bridge pier is the prime cause for most of the bridge failures. The main objective of the present study was to investigate the flow behavior and the scour phenomenon around the bridge piers. Moreover, the numerical simulations were even carried out using CFD- Fluent, k –epsilon turbulence model, to elaborate the physics behind the scour formation. In the present study, scour depth was estimated making use of well known empirical formulae. Further, it was also determined experimentally for two plan shapes of bridge piers viz., circular and oblong. The experimental results were in good consonance with the empirical formulae. The simulation results for dynamic and static pressures along with the velocity magnitude profiles, showed good similarities with the experimental results. Hence, CFD simulation tool can be used for wide understanding of the flow behavior around the bridge piers even without physical model studies.*
Keywords – *bridge pier, fluent, k-epsilon, scour*

Date of Submission: 12-09-2018 Date of acceptance: 27-09-2018

I. INTRODUCTION

Scour is the engineering term for the erosion caused by water on the soil nearby any hydraulic structure. Scouring phenomenon is a very complex problem as many parameters such as flow depth, velocity, shape of pier, size of pier, types of bed materials etc control the scouring. Scouring in bridge piers occurs due to the formation of horse shoe vortex forming in front of the pier. Due to this phenomenon, the bed material dislocates which results in scour. Scour can be either caused by the normal flow or flood events. The boundary layer in the flow past a bridge element undergoes a 3D separation. This separated shear layer rolls up along the obstruction to form a vortex system in front of the element which is swept downstream by the river flow. The formation of the horseshoe vortex and the associated down flow around the bridge element results in increased shear stress. Hence, an increase in sediment transport capacity of the flow occurs. This leads to the development of a deep hole (scour hole) around the bridge element. The formation of the scour hole changes the flow pattern causing a reduction in shear stress by the flow and a consequent reduction in the sediment transport capacity. Scour can occur under any flow condition that makes the bed mobile within the vicinity of the obstruction. However, the rate of scouring is much higher when the flow is larger. The void or depression left behind, as sediment is washed away from a stream or river bed is called as scour hole. The flow and scour pattern around a circular pier is detailed in **Fig. 1**.

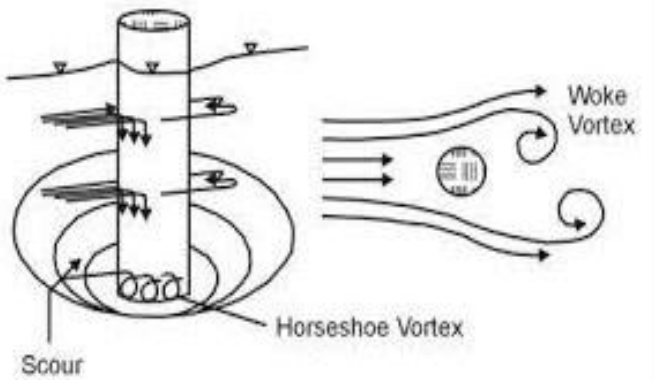

Fig. 1 horse shoe vortex formation (source: HEC-18, (2012))

The strong vortex motion caused in the presence of the pier, entrains bed sediments in the vicinity of the pier base. The down flow rolls up as it continue to make a hole, and through interaction with the incoming flow develops into a complex vortex system. The vortex then extends downstream laterally to the sides of the pier. This vortex is often referred to as horseshoe vortex because of its resemblance to a horseshoe. Thus, the horseshoe vortex developed as a result of flow separation at the upstream face of the pier being excavated by the downstream flow [1].

Significant erosion of the bed takes place at different scales and may be classified on this basis as degradation, general scour or local scour.

Degradation is a regional phenomenon which involves progressive and sustained lowering of the bed over long distances and long time spans. Channel degradation occurs when the rate of sediment input from upstream cannot match with the sediment transport rate along the channel. This occurs at a steepened reach with a high energy level that may be called as a nick point or a head cut, and it leads to the sediment being scoured from the bed. In a flume, degradation is observed in the experiment concerned with bed forms. Under upper bed form regime conditions, when the rate of sediment input from the header tank cannot match the high transport rate in the steep channel, scour extends down to the solid bed of the flume.

General scour is a site specific phenomenon which involves the lowering of the bed in a reach, either progressively over a long period or only during high flow events. Usually, general scour is caused by the acceleration of the flow velocity due to contraction of the width by either bridge abutments or by river training works such as dikes, groynes, vanes, guide walls or other hard structures.

Local scour is local phenomenon which involves the lowering of a portion of the bed due to locally increased velocities and turbulence levels around a solid obstruction to the flow. It is usually associated with bridge piers, dikes, revetments, flow diversions and most other hydraulic structures [2].

The main scope of the present study was to investigate the intensity of scour development around bridge piers. This was carried out using analytical and physical models. Consequently, the experimental results were used to simulate using ANSYS-CFD to ascertain the ideal of shape for the bridge piers.

Experimental studies on the bridge scouring were carried out by a large number of researchers, especially in the field of non cohesive bed condition. **Wen Xiong et al,** (2017) proposed 3D simulation method for the live-bed bridge scour considering suspended sediment loads. The k-ε model was used to predict the effects of turbulence and to simulate the regular flow field (away from the piers) at the bridge site [3]. **Ghasemi et al,** (2017) studied the comparisons between the simulated and observed scour depths, and concluded that these were underestimated by 30% to 20% for upper and lower parts of the pier [4]. **Wen Xiong et al** (2016) conducted another form of simulations for bridge scour using an Eulerian two-phase flow model. The study was conducted to evaluate the parametric analyses using two-phase flow model. This part of the study investigated the impacts of environmental and design parameters, on the characteristics of scour developments [5]. **Sreedhara et al,** (2016) investigated the variations in velocity and pressure field of the fluid domain. The RANS equations were adopted to model the boundary between the three phases, viz., water-air and water-sediments in which the Land surface model (LSM) was adopted. The author concluded that there was significant effect of pier shape on the velocity profile, mechanism and magnitude of local scour [6]. **Wen Xiong et al** (2014) simulated the turbulent flow around the vertical circular piers for clear water to describe the 3D scour behavior around the piers of bridges. The transient shear stress was estimated by k-ε turbulence model considering shear stress as a key parameter to judge the sediment incipient motion in scour process [7].

Aghaee et al, (2010) carried out a 3D numerical simulation to study the turbulent flow around a vertical circular pier. The study adopted fully developed hydrodynamic equations viz., Reynolds Averaged Navier-Stokes equations (RANS) and Space Averaged Navier-Stokes equations. The numerical model results showed that the length and intensity of the wake and the horseshoe vortices were mainly affected with the turbulence models used [8]. **Vasquez** et al, (2009) investigated the qualitative simulations of local scour in complex bridge piers under tidal flow using Flow-3D model. The model was evaluated by the application of the Fractional Area Volume Method (FAVOR) for scour development in a complex pier made of 10 cylindrical piles. The CFD model was found to be a good hydraulic design tool for complex piers [9]. **Wenrui et al,** (2009) investigated the scale effects on turbulent flow and scour around bridge piers. The appropriate scour equation was developed for HEC-18 from the laboratory experiments carried out in a relatively small scale. The physical scale and boundary velocity were set up using 3D CFD model, based on the Froude's similarity law to determine the sediment scour. The CFD simulation employed was a 2nd order turbulent model for calculating turbulent velocity and sediment scour [10].

From the above literature, it is evident that the numerical simulations play a significant role in broad understanding of the scour phenomenon and its constituent parameters. The present study was carried out to

evaluate empirically, experimentally and numerically, to compare various features of scour around the bridge piers.

II. METHODOLOGY

Scour is due to erosive action of flowing water to excavate and dislocate the material from the bed, banks, and abutments. Different bed materials will scour at different flow rates. Scour can be deepest at times of peak flood, but hardly visible as floodwater recede leading to filling-up of scour holes with sediment.

As the first step, the sieve analysis was conducted to get the grain size distribution for the medium (sand) adopted for the experiments. Specific gravity test was also conducted using pycnometer apparatus. It was observed that the bed was in motion from the shield's diagram. The temperature of the re-circulating water was taken as 27.5°C and the corresponding kinematic viscosity was found to be 8.5175 x 10^{-7} m^2/sec. The average bed shear stress, shear stress due to grains, and bed forms [11] for the flow were estimated using equation (1).

$$\left.\begin{aligned} &\tau_0 = \gamma RS_0, \tau_0^{'} = \left(\frac{n_s}{n}\right)^{\frac{3}{2}} \gamma RS_0 \\ &\tau^{''} = \tau_0 - \tau_0^{'} \end{aligned}\right\} \quad \ldots\ldots\ldots\ldots\ldots\ldots (1)$$

Where, τ_0 is average bed shear stress due to flow, γ is unit weight of water, R is hydraulic mean radius, S_0 is slope of channel, $\tau_0^{'}$ is shear stress due to grains, $\tau_0^{''}$ is shear stress due to bed forms, n is Manning's roughness coefficient of the channel flow, n_s is Manning's roughness coefficient corresponding to the grain roughness only

The sand bed particle movement was evaluated based on the shear Reynolds number (R_*), and Shield entrainment functions as detailed in equation (2).

$$\left.\begin{aligned} &V_* = \sqrt{\frac{\tau_0}{\rho}}, R_* = \frac{V_* d}{\nu} \\ &\frac{\tau_0}{(s-1)*\gamma_d} \end{aligned}\right\} \quad \ldots\ldots\ldots\ldots\ldots\ldots (2)$$

Where, V_* is shear velocity, ρ is the density of water, d is the diameter of particle, s is specific gravity of sediment, ν is kinematic viscosity,

The bed material characterization was made as washed out dunes or said to be in transition, based on the regime criterion equation (3) from the regime flow graph.

$$S* = \frac{S_O}{\left(\frac{\gamma_S}{\gamma} - 1\right)}, \frac{R}{d} \quad \ldots\ldots\ldots\ldots\ldots\ldots (3)$$

The scour depths were evaluated using HEC[1] and Colorado State University[12] equation (4), prescribed by different researchers for comparison with the experimental analysis.

$$\left.\begin{aligned} &\frac{y_s}{y_1} = 2.0 K_1 K_2 K_3 \left(\frac{a}{y_1}\right)^{0.65} (F_r)^{0.43} \\ &\frac{d}{y_1} = 2.0 K_1 K_2 K_3 K_4 \left(\frac{b}{y_1}\right)^{0.65} (F_r)^{0.43} \end{aligned}\right\} \quad \ldots\ldots\ldots\ldots\ldots\ldots (4)$$

Where, y_s (or) d is scour depth (m), y_1 is upstream depth of flow (m), K_1 is correction factor for the bridge deck shape (ranged between 0.9-1.1), K_2 is the correction factor of flow hit angle with bridge pier, K_3 are correction coefficient of bed, K_4 is coefficient used when a cover layer is formed on scour hole, b / a is bridge pier width (m), and F_r is Froude number upstream of bridge pier.

Experimental Analysis:

The experiments were carried out in the Fluid Mechanics Laboratory of Department of Civil Engineering, College of Engineering (A), Osmania University, Hyderabad**.** The experiments were conducted in a recirculating flume of 2.0 m length, 1.0 m width and 0.02 m depth with a collecting tank of 1.0 m x 0.8 m x 0.63 m. The flume has a working section filled with sand sediments to a uniform thickness of 0.17 m. The schematic diagram of the experimental setup along with plan and elevation are shown in **Fig. 2**. The entrance zone was facilitated with small pebbles for smooth, uniform and channelized flow. The inlet gate of the flume

was having a dimension of 10.0 cm x 10.0 cm x 0.05 cm. The flume is supplied with 0.37 kW, centrifugal pump located at upstream of the flume. The channel was set at a slope of 4%, and a channel of 10.0 cm wide and 2.0 cm deep was prepared. The flow rate was set to 5 lpm. Initially the flow was allowed into the channel for 30 minutes. The sediment yield and channel discharge were observed for consistency. The experiments were conducted using two shapes of bridge piers viz., circular and oblong. The circular pier was of 25 mm diameter and 125 mm height, while oblong pier was having a length of 125 mm length and a width of 25 mm. The bridge piers were placed at a distance of 1.0 m from the inlet gate of the flume.

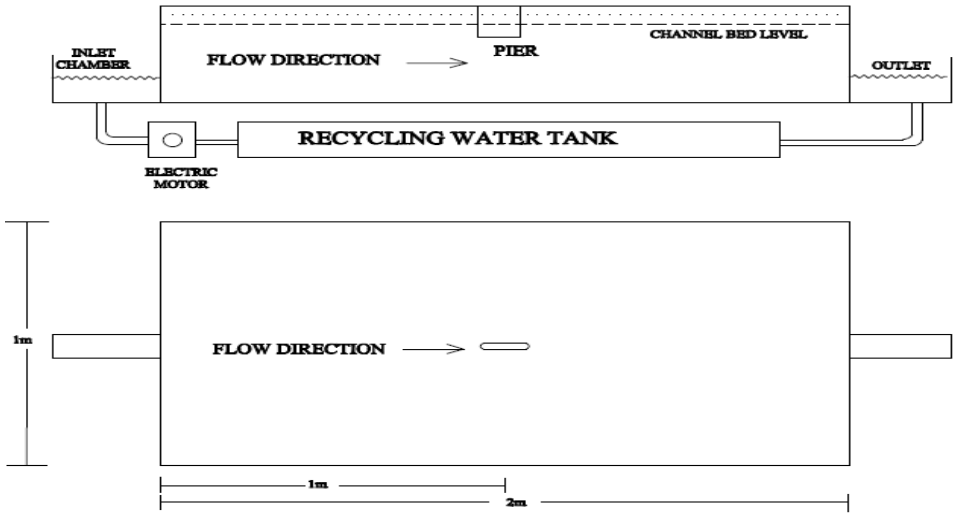

Fig. 2 plan and elevation of experimental setup

From the physical study, maximum scouring pattern was observed to develop on the right and left sides of the pier. At the downstream side, a simple ripple formation was noticed. The scouring process for the first 70 minutes was very critical as more than 70% of scouring developed during this time. A symmetrical scour hole was observed after 120 minutes. The maximum scour hole was found on the upstream (inlet) left and right sides. Moreover, a small heap of deposition was found on the downstream of the pier as shown in **Fig. 3**. The salient features of experimental studies adopted for the two bridge piers is elaborated in **Table 1**.

Table 1 Salient features and results of the tests

Parameter	Circular pier	Oblong pier
Velocity (m/sec)	0.041	0.041
Hydraulic radius	0.0568	0.0568
Reynolds number	582	582
Froude number	0.09	0.09
Scour depth at downstream side pier (mm)	5.6	5.2
Scour depth at upstream side of pier(mm)	8.6	8
Scour depth at right side of the pier(mm)	12.5	9.8
Scour depth at left side of the pier(mm)	11.5	9.3

Simulation Process:

The numerical modeling technique ANSYS – CFD (Fluent) was adopted for the present study. The analysis was carried out using Finite Volume Method (FVM) by k-Epsilon and k-Omega turbulence models. As a first step, the geometry (2D) of the experimental setup for circular pier as detailed in the **Fig. 4** was generated in ANSYS – Workbench. The same procedure was followed for oblong pier also.

Fig. 3 scour formation for circular and oblong pier

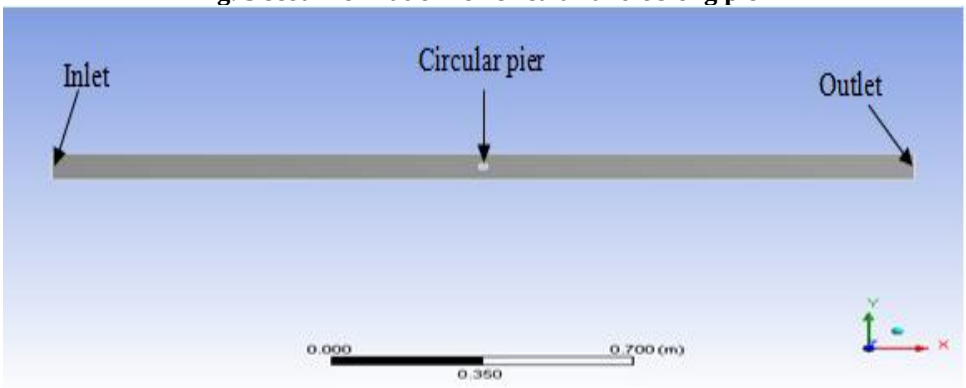

Fig. 4 geometry of the circular pier

Subsequently, the mesh was generated for both the piers. In the mesh generation, edge sizing and refinement methods were used. The edge sizing number of divisions was about 50 around the circular and oblong piers. The refinement in the mesh was made to accurately simulate the results around the piers as shown in **Fig. 5**. The coarser mesh was adopted away from the pier boundaries covering whole domain of channel. In the next step of simulation, the mesh was imported into the fluent solver analysis adopted different turbulent models.

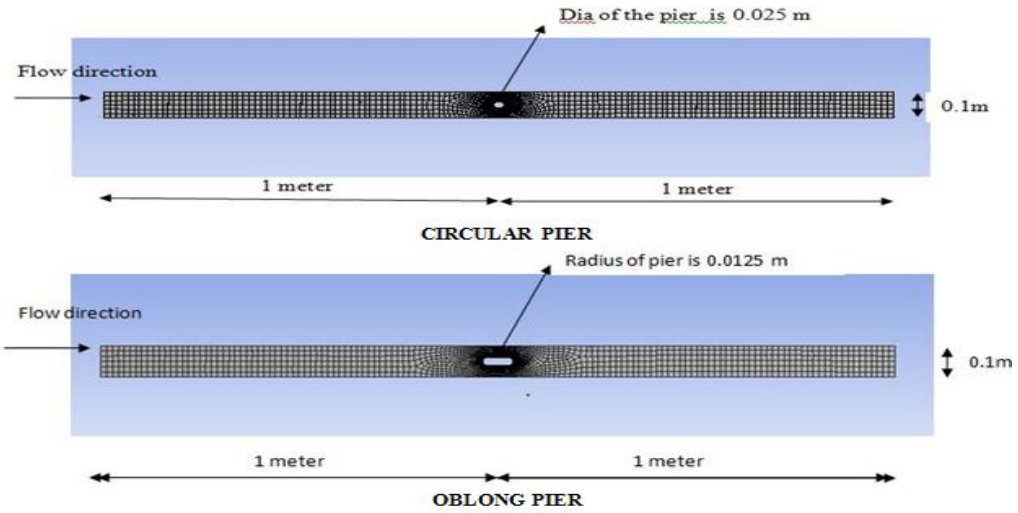

Fig. 5 meshing of circular and oblong piers

For the two dimensional steady state incompressible flows the Reynolds - Averaged Navier-Stokes equations play a vital role as defined in equation (5). The approach involves solving two differential equations, one representing the generation of transport of turbulence and the other representing the transport of dissipation of turbulence viz., k - ε and k – ω models adopting the Turbulence Kinetic Energy and the Dissipation Rate for

epsilon and omega as detailed in the equation (6) [13]. The results of the simulated parameters are highlighted in **Table 2** and the corresponding details of the experimental setup are shown in **Fig. 6**. The solution was run for the time step(s) of 0.01s and has converged after 1447 time steps as detailed in **Fig. 7**.

$$\left.\begin{aligned}&\frac{\partial \bar{u}}{\partial x}+\frac{\partial \bar{v}}{\partial y}=0\\ &\rho\left(\bar{u}\frac{\partial \bar{u}}{\partial x}+\bar{v}\frac{\partial \bar{u}}{\partial y}\right)=-\frac{\partial \bar{p}}{\partial x}+\frac{\partial}{\partial x}\left(\mu\frac{\partial \bar{u}}{\partial x}-\rho u'u'\right)+\frac{\partial}{\partial y}\left(\mu\frac{\partial \bar{u}}{\partial y}-\rho u'v'\right)\\ &\rho\left(\bar{u}\frac{\partial \bar{v}}{\partial x}+\bar{v}\frac{\partial \bar{v}}{\partial y}\right)=-\frac{\partial \bar{p}}{\partial y}+\frac{\partial}{\partial x}\left(\mu\frac{\partial \bar{v}}{\partial x}-\rho u'v'\right)+\frac{\partial}{\partial y}\left(\mu\frac{\partial \bar{v}}{\partial y}-\rho v'v'\right)\end{aligned}\right\} \qquad (5)$$

$$\left.\begin{aligned}&\frac{\partial k}{\partial t}+U_j\frac{\partial k}{\partial x_j}=\tau_{ij}\frac{\partial U_i}{\partial x_j}-\varepsilon+\frac{\partial}{\partial x_j}\left[(v+v_T/\sigma_k)\frac{\partial k}{\partial x_j}\right]\\ &\frac{\partial \varepsilon}{\partial t}+U_j\frac{\partial \varepsilon}{\partial x_j}=C_{e1}\frac{\varepsilon}{k}\tau_{il}\frac{\partial U_i}{\partial x_j}-C_{e2}\frac{\varepsilon^2}{k}+\frac{\partial}{\partial x_j}\left[(v+v_T/\sigma_\varepsilon)\frac{\partial k}{\partial x_j}\right]\\ &\frac{\partial \omega}{\partial t}+U_j\frac{\partial \omega}{\partial x_j}=\alpha\frac{\omega}{k}\tau_{ij}\frac{\partial U_i}{\partial x_j}-\beta\omega^2+\frac{\sigma_d}{\omega}\frac{\partial k}{\partial x_j}\frac{\partial \omega}{\partial x_j}\left[\left(v+\sigma\frac{k}{\omega}\right)\frac{\partial \omega}{\partial x_j}\right]\end{aligned}\right\} \qquad (6)$$

Table 2 Boundary conditions of the piers

Section	Circular pier Boundary Conditions	Oblong pier Boundary conditions
Inlet	Velocity Inlet Velocity = 0.041 m/sec Turbulence Intensity, I = 7.219 Hydraulic Diameter (4R) = 0.0568 m	Velocity Inlet Velocity = 0.041 m/sec Turbulence Intensity, I = 7.219 Hydraulic Diameter (4R) = 0.0568 m
Outlet	Pressure outlet	Pressure outlet
Channel Walls	Wall (Stationary) with no slip Condition Roughness height = 0.0mm Roughness constant = 0.5	Wall (Stationary) with no slip Condition Roughness height = 0.0mm Roughness constant = 0.5
Pier Walls	Wall (Stationary)	Wall (Stationary)

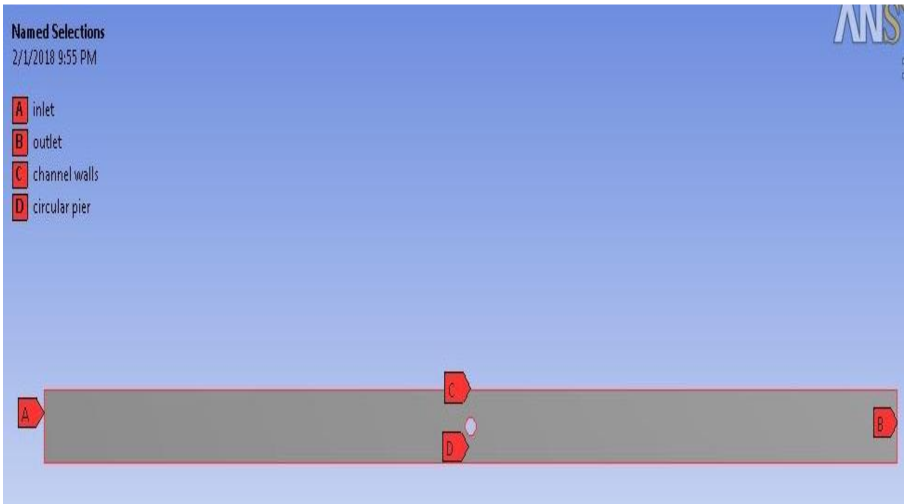

Fig. 6 boundary conditions for circular pier

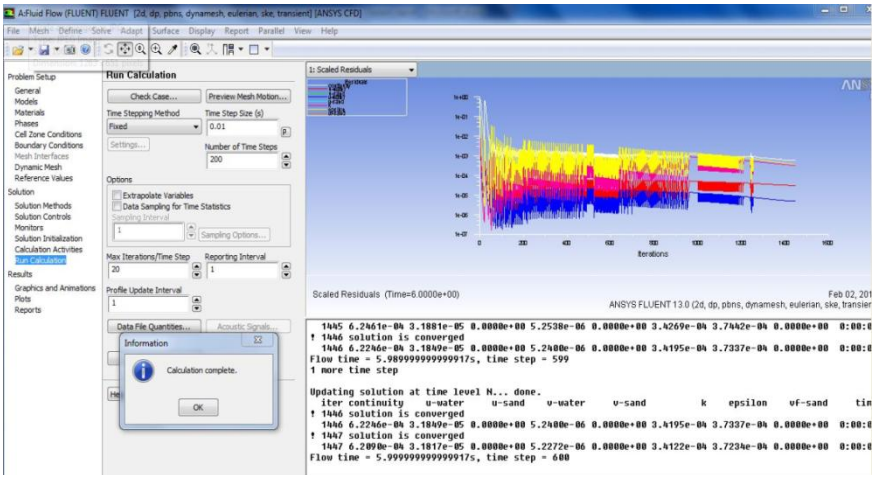

Fig. 7 iteration graph

III. RESULTS

The present study was carried out in the three different phases and the following results were deduced.

1. The median size of the particle (d_{50}) was estimated as 0.90 mm by sieve analysis as detailed in **Fig. 8** and the specific gravity was estimated as 2.54 by pycnometer test.

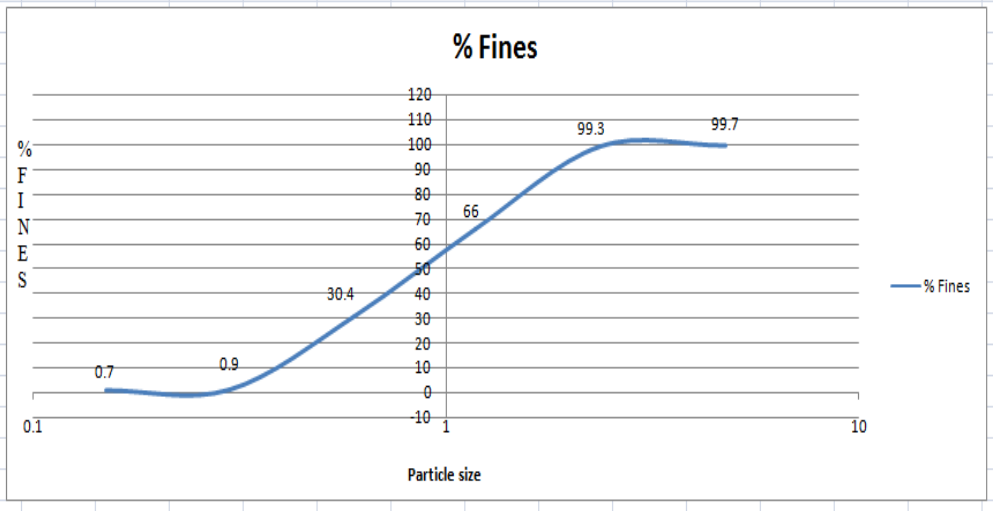

Fig. 8 sieve analysis

2. For the discharge of 8.33×10^{-5} cumec the Reynolds number obtained was 582 confirming the flow to be turbulent and Froude's number was 0.13 inferring the flow to be subcritical.
3. The average bed shear due to flow was estimated to be 5.57 N/m^2 from the equation (1).
4. The shield entrainment function was evaluated as 0.40 from the equation (2) based on the average shear stress value, indicating that the particles are in motion.
5. The shear stress due to the grains was estimated as 0.062 N/m^2 and the shear stress due to bed forms as 5.509 N/m^2.
6. The scour depth values from the experiment analysis and empirical calculations based on the HEC and CSU formulae, equation (4) are detailed in **Fig. 9**. It was observed that both the empirical formulae gave the same scour depth of 14.17 mm. The variation between the empirical formulae and the experimental values was found to be around 2.6%. This variation could be because of error in experimentation.

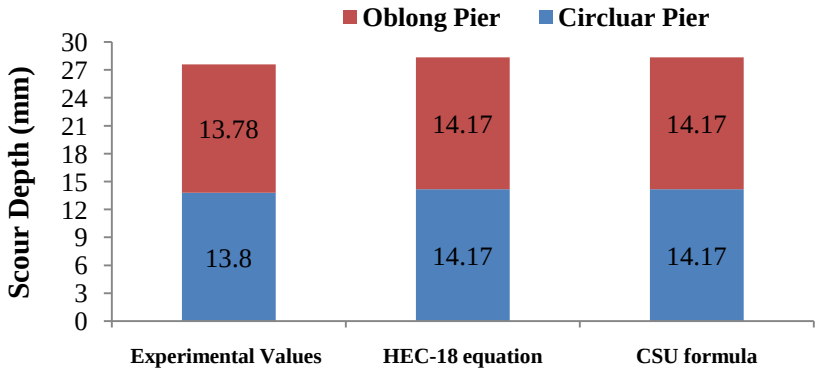

Fig. 9 comparative results

7. The contours of velocity magnitude were plotted for two turbulence models namely k-epsilon and that, k-omega for circular pier is shown in **Fig. 10.** It was observed from the simulation, that the velocity magnitude value was in clear consonance with the experimental value of $4.1x10^{-2}$ m/sec.

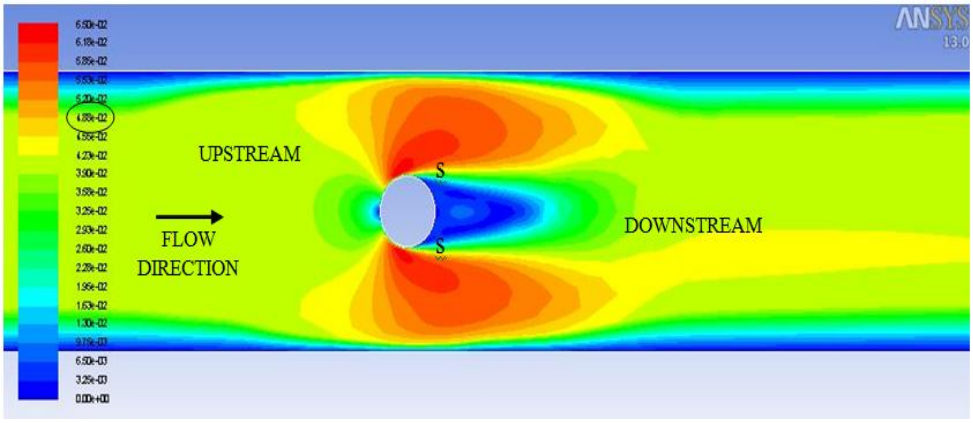

Fig. 10 velocity contours for circular pier (s-separation)

8. It was deduced from the simulation that, the maximum velocity of $6.5x10^{-2}$ m/s for circular and $6.33x10^{-2}$ m/s for oblong occurred at the section where the stream lines were practically parallel as shown in **Fig. 11**. The variation was less on upstream left and right sides of the piers.
9.

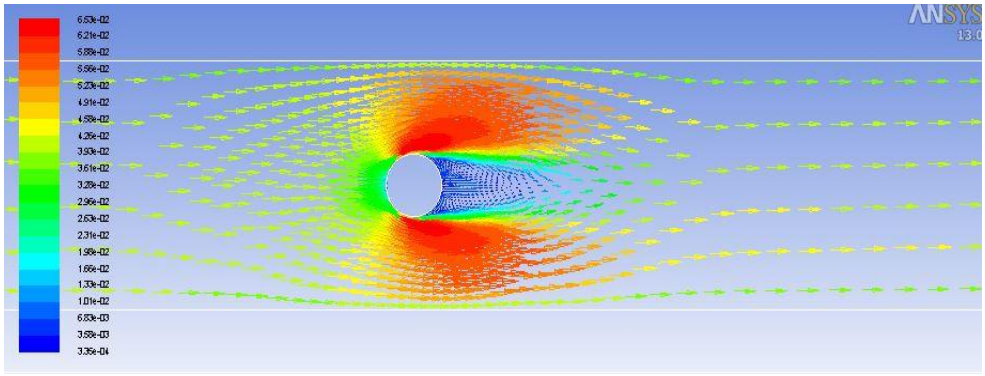

Fig. 11 velocity vector around the circular pier

10. The contours of static pressure were plotted for both the turbulence models to understand the profile variation around the circular and oblong piers as shown in **Fig. 12**. From the figure it is clear that, the pressure is maximum at the stagnation point and gradually decreases along the front half of the cylinder.

The flow remains attached in the favourable pressure region. However, in the presence of a strong viscous force, as the pressure starts to increase in the rare half of the cylinder, the particles experience an adverse pressure gradient. The fluid particles will tend to move against the increasing pressure force. Therefore,

the fluid particles could not be stopped or reversed, causing the neighbouring particles to move away from the surface. This phenomenon is known as boundary layer separation.

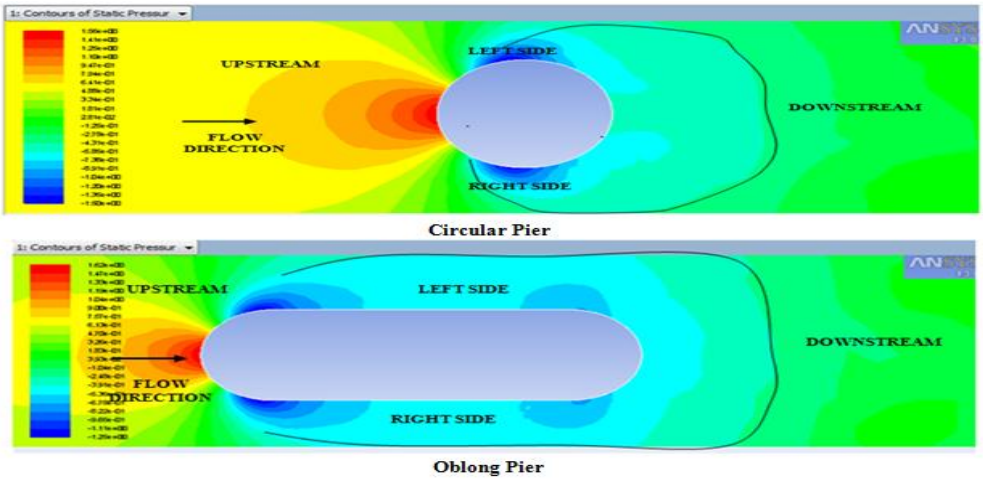

Fig. 12 contours of static pressure

11. The contours of dynamic pressure were plotted for both the turbulence models to understand the profile variation of dynamic pressure around the circular and oblong piers as shown in **Fig. 13**. The dynamic pressure was obtained as 0.844 Pa (green colour) from the simulation and from the analytical estimations as 0.844 Pa. Both the values were observed to be in good agreement with each other.

It is evident from the figure that, as the flow separates from the surface of the cylinder, creates a highly turbulent region behind the cylinder called as wake. The pressure inside the wake region remains low and nearly constant. As the flow separates, a net pressure force (pressure drag) is produced.

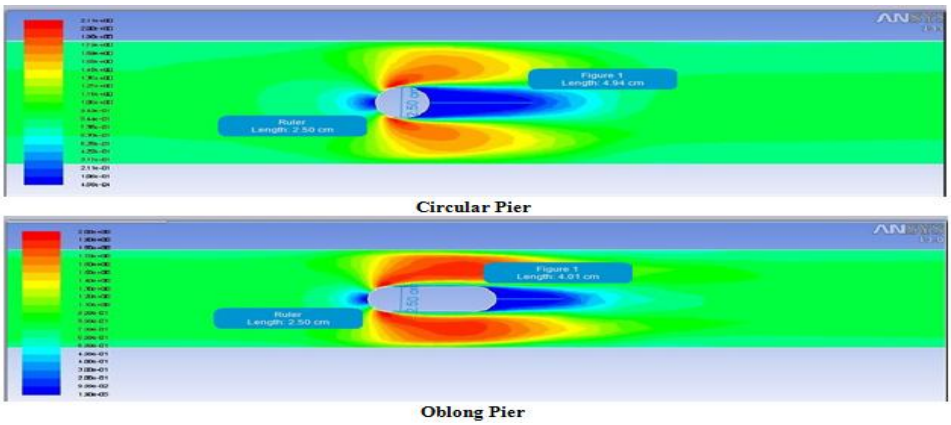

Fig. 13 contours of dynamic pressure.

IV. Conclusions

In the present study, scouring process around the bridge piers was empirically and experimentally investigated for two different plan shapes of bridge piers viz., circular and oblong. The present study reaffirms that, horseshoe vortex formation is the main causative factor for bridge scour. Most of software packages dealing with the dynamics of fluid flow are developed based on the basic governing equations. Considering the difficulty and the expenditure on the construction of the experimental setups, the use of software packages is gaining due importance for the in depth understanding of particle movement.

In the present study, commercial software namely ANSYS-FLUENT was used for the elaborate understanding of the scouring phenomena. The present numerical analysis mainly focuses on the variation of velocity, turbulent kinetic energy and dynamic pressures. Moreover, it is observed from the present study that, as time increases scour depth will increase and reaches an equilibrium state, beyond which increase in scour depth was negligible. The following conclusions were drawn from the present study:

1. From the present study, it is observed that the scour depth was approximately same for both the plan geometries viz., circular and oblong.

2. The experimentation process was carried out for about one and half hour. Scouring was noticed on right and left side of the both the piers. However, the maximum scour was observed to form in the first 30 min.
3. From simulation studies, it was observed that the stagnation points were formed on the downstream side for both circular pier and oblong piers. The region of wake extended to a length of 4.94 cm and 4.01 cm respectively for circular and oblong piers.
4. The velocity magnitudes, turbulent kinetic energy and dynamic pressure values from the simulated results were reasonably matching with the analytical values for both the turbulence models via, k-ε and k-ω.

REFERENCES

[1]. Arneson L.A., Zevenbergen L.W., P.F. Lagasse, P.E. Clopper, Evaluating Scour at Bridges, Publication No. FHWA-HIF-12-003 U. S. Department of Transportation Federal Highway Administration, 2012, http://www.fhwa.dot.gov.

[2]. HEC 18 (2012) - www.fhwa.dot.gov/engineering/hydraulics/pubs/hif12012.

[3]. Wen Xiong, Pingbo Tang, Bo Kong and C. S. Cai, Computational Simulation of Live Bed Bridge Scour Considering Suspended Sediment Loads, Journal of Computing in Civil Engineering, ASCE, 31(5), 2017, [04017040]. DOI: 10.1061/(ASCE)CP.1943-5487.0000689.

[4]. Ghasemi M and Soltani-Gerdefaramarzi S, The Scour Bridge Simulation around a Cylindrical Pier Using Flow-3D, Journal of Hydro sciences and Environment, 1(2), 2017, 46-54.

[5]. Wen Xiong, Pingbo Tang, Bo Kong and C. S. Cai, Reliable Bridge Scour Simulation Using Eulerian Two-Phase Flow Theory, Journal of Computing in Civil Engineering,CP.2016, 1943-5487.0000570.

[6]. Sreedhara B M, Sanooj A, Manu , S Mandal, Simulation of Local Scour around Circular and Round Nosed Bridge Pier using REEF3D, International Journal of Innovative Research in Science, Engineering and Technology, 5(9), 2016, 149 – 154.

[7]. Wen Xiong, C. S. Cai, Bo Kong, and Xuan Kong, CFD Simulations and Analyses for Bridge Scour Development Using a Dynamic-Mesh Updating Technique, Journal of Computing in Civil Engineering, 30(1), 2014, DOI:10.1061/(ASCE)CP.1943-5487.0000458.

[8]. Aghaee Y and Hakimzadeh H., Three Dimensional Numerical Modeling of Flow around Bridge Piers Using LES and RANS: River flow, Dittrich, Koll, Aberle & Geisenhainer (eds) Bundesanstalt für Wasserbau, 2010, 221-218.

[9]. J. A. Vasquez, and B. W. Walsh, CFD simulation of local scour in complex piers under tidal flow: 33rd IAHR Congress, Water Engineering for a Sustainable Environment, International Association of Hydraulic Engineering & Research (IAHR), 2009.

[10]. Wenrui Huang, Qiping Yang and Hong Xiao, CFD modeling of scale effects on turbulence flow and scour around bridge piers, Journal of Computing in Civil Engineering, 38(5), 2009, 1050 – 1058.

[11]. Subramanya K, "Flow in open channels" –Third edition-McGraw Hill Publication, 2009, 491-493.

[12]. Fatemeh Mousavi1, Rasoul Daneshfaraz, Evaluating Various Factors in Calculation of Scour Depth around Bridge Piers using HEC- RAS Software, CSU2001 and Froehlich Equations, Journal of Civil Engineering and Urbanism, 3(6), 2013, 398-402.

[13]. Wilcox, David C. Turbulence Modeling for CFD, DCW Industries, Inc. California, 2006.

Prasanna S V S N D L and Suresh Kumar, N "Simulation of Flow Behaviour around Bridge Piers Using ANSYS – CFD "International Journal of Engineering Science Invention (IJESI), vol. 07, no. 09, 2018, pp.13-22